Theoretical Accuracy Analysis of Indoor Visible Light Communication Positioning System Based on Received Signal Strength Indicator

Xueli Zhang, Jingyuan Duan, Yuegang Fu, and Ancun Shi

***Abstract*—This paper analyzes an indoor positioning system using white lighting LEDs. The performance of the positioning system is determined by the layout of LEDs, the receiver circuit, incidence angle of light, LED light source, and the photodiode. The Cramer–Rao bound as the theoretical accuracy limitation of received signal strength indicator algorithm is derived. The influences to positioning accuracy of multipath reflections and unparallel optical axis of LEDs and receivers are analyzed in certain scenarios. It is concluded that if the diffuse channel gain is measured previously in a certain environment and the modulation speed is far less than the channel cutoff frequency, the theoretical accuracy limit is not affected by multipath link. Multiple noises of system are analyzed in detail. The influence to positioning accuracy of indoor uniform illumination is also discussed. The result proves that the theoretical estimated accuracy of triangular LEDs array is higher than square LEDs array. With typical parameter values, the simulated theoretical accuracy of system is up to the level of centimeter.**

***Index Terms*—Cramer–Rao bound, multipath reflection, positioning accuracy, received signal strength indicator, Sparrow's criterion, visible light communication.**

I. Introduction

With the rapid development of solid state lighting technologies, the light-emitting diodes (LEDs) will replace the traditional light sources and become a dominant role in the lighting market. [1], [2]. LEDs are also applied to communication and positioning systems because of the modulation characteristics which has been an attractive research topic [3], [4]. Different technologies are available and have been studied for indoor positioning such as infrared, ultrasound, laser, radio frequency (RF) and so on. Compared with these techniques, visible light communication (VLC) positioning technology based on illumination LEDs has higher positioning accuracy. Some papers indicated that VLC positioning system can reach centimeter accuracy by simulation [5].

Manuscript received January 23, 2014; revised June 27, 2014; accepted August 12, 2014. Date of publication August 18, 2014; date of current version September 17, 2014. This work was supported by the National Key Basic Research Program of China (973 Program) under Grant 2013CB329205 and the Natural Science Foundation of China under Grant 61375083.

X. Zhang is with the Optoelectronic System Laboratory, Institute of Semiconductors, Chinese Academy of Sciences, Beijing 100083, China and also with the Changchun University of Science and Technology, Beijing 100044, China (e-mail: zhangxueli@semi.ac.cn).

J. Duan and A. Shi are with the Optoelectronic System Laboratory, Institute of Semiconductors, Chinese Academy of Sciences, Beijing 100083, China (e-mail: jyduan@semi.ac.cn; sacthy@semi.ac.cn).

Y. Fu is with the Institute of Optical Engineering, Changchun University of Science and Technology, Changchun 130022, Jilin, China (e-mail: fuyg@cust.edu.cn).

Digital Object Identifier 10.1109/JLT.2014.2349530

Most of the published works analyzed the indoor positioning accuracy through simulation or experiment. However, the discussion of theoretical accuracy of VLC positioning system is rarely mentioned. Only one article calculated the theoretical accuracy limitation of VLC time of arrival (TOA) algorithm by deriving the Cramer–Rao bound (CRB) using intensity modulated windowed sinusoidal signals [6]. But there is no theoretical accuracy analysis of indoor VLC positioning system based on received signal strength indicator (RSSI) algorithm. Besides, little research has been done to analyze the influence to VLC positioning accuracy of different LEDs layout. In addition, the work of analyzing the influence to positioning accuracy of diffuse link and unparallel optical axis of LEDs and detectors has not been seen in published papers. To obtain a VLC positioning system with better performance, which is required in many applications, more work about the positioning accuracy should be done.

In this paper, the expression of CRB based on VLC RSSI algorithm is derived at first. The influence to positioning accuracy of multipath reflections is considered. Two 2-D cases where an angle exists between detector plane and floor plane are analyzed. Then the RSSI positioning system based on white lighting LEDs is described. The system noises are analyzed in detail. Sparrow's criterion is used to analyze the uniform illumination under different layout of LEDs. At last, we give a numerical simulation of CRB with a range of typical parameter values and the influences of parameters are gotten. The results show that the CRB in the level of centimeters could be achieved with typical parameter values. This gives a significant prospect to the accurate indoor positioning application based on VLC RSSI algorithm.

II. Cramer–Rao Bound

We adopt the RSSI algorithm to obtain distance between transmitter and receiver. Like radio positioning technologies, we call the LED sources used for positioning base stations (BSs) and the object needed to locate is mobile station (MS). After least three distances are obtained between BSs and MS, the MS coordinate could be estimated by triangulation algorithm. Therefore, only the distance estimation is discussed in this paper.

Accuracy limitations of ultra-wideband or RF wireless systems can be analyzed precisely by means of the CRB [7]–[9]. But the results cannot be directly utilized for the VLC system because the intensity distribution model of VLC is different from RF drastically and visible light is unable to bypass the opaque obstacles like RF.

0733-8724 © 2014 IEEE. Personal use is permitted, but republication/redistribution requires IEEE permission.
See http://www.ieee.org/publications_standards/publications/rights/index.html for more information.

A. Optical Channel

For optical channel with impulse response $h(t)$, the received signal current $Y(t)$ can be expressed as

$$\begin{aligned} Y(t) &= R \cdot x(t) \otimes h(t) + N(t) \\ x(t) &= \frac{C}{2}.\cos(2\pi f_1 t) \end{aligned} \tag{1}$$

where *R* is the photodiode responsivity, C is peak-to-peak (pk-pk) optical power of modulated LED source, $N(t)$ is the white Gaussian noise with mean μ and variance σ^2, and the symbol $\otimes$ denotes convolution. In this paper, we transmit a modulated cosine signal, whose modulation frequency f_1 is below 4 MHz and initial phase is treated as zero.

Based on the similarity between visible light and infrared light, the line-of-sight (LOS) and diffuse links are considered. The channel gain is given by [10]

$$H(f) = \eta_{LOS} + \eta_{\text{diff}} \frac{e^{j2\pi f \Delta T}}{1 + j\frac{f}{f_0}} \tag{2}$$

where f_0 is the cutoff frequency, ΔT describes the delay between the LOS signal and the onset of the diffuse signal.

We select S2744-08 photodiode of Hamamatsu Photonics, whose sensitive area is 0.2 cm^2. Only plaster walls are considered in this paper. The reflectivity of visible light and near-infrared on plaster walls which are almost similar is about 0.7–0.85. According to the definition of f_0, we can adopt the same value as [10], [11]. Therefore, we can use the conclusion of [10] that the channel gain is almost flat under the frequency of 10 MHz. In addition, ΔT will be similar for visible light and near-infrared in same given indoor scenario. [10] gave the most worse ΔT 20 ns. ΔT might be far less than modulation cycle of $x(t)$ in this paper, which means diffuse signal has little effect on the phase of LOS link. Thus, the channel gain with modulation frequency of f_1 can be expressed as $H(0)$. We can get

$$\begin{aligned} H(f_1) &= H(0) = \eta_{LOS} + \eta_{\text{diff}} \\ &= \frac{(m+1)A_R}{2\pi d^2}\cos^m(\phi)\cos(\varphi) + \frac{A_R}{A_{\text{room}}}\frac{\langle\rho\rangle}{1-\langle\rho\rangle} \end{aligned} \tag{3}$$

where A_R is detector effective area, ϕ is the angle of irradiance with respect to the transmitter perpendicular axis, φ is the angle of incidence with respect to the receiver optical axis, the number of m depends on the order of approximate Lambertian model, A_{room} is room surface, $\langle\rho\rangle$ express the average reflectivity of a given room.

The average reflectivity in a given environment can be measured. Thus, η_{diff} can be treated as a constant.

B. The Derivation of CRB

Let $\mathcal{B} = \{1, 2, \ldots, B\}$ be the set of indices of all BSs involved whose locations are already known. The value of *B* is greater than three. We define a *B*-dimensional vector θ:

$$\theta = (\, d_1 \quad \cdots \quad \cdots \quad d_B \,)^T \tag{4}$$

where d_b is the distance between b_{th} BS and MS for $\mathrm{b} \in \mathcal{B}$. Let all LEDs involved match Lambertian model and have identical mode number m. BSs are installed on the ceiling and pointing down. The MS setup is placed at a vertical distance *h* below the ceiling which is facing up with a small angle.

Let perpendicular axis of LEDs and of receivers equal. (3) can be converted as

$$H(0) = \frac{(m+1)A_R h^{m+1}}{2\pi d^{m+3}} + \frac{A_R}{A_{\text{room}}}\frac{\langle\rho\rangle}{1-\langle\rho\rangle}. \tag{5}$$

We assume the optical filter with ideal band-pass which causes no loss in the pass-band and completely blocks any optical frequencies in the stop-band. The CRB states that the inverse of Fisher Information Matrix (FIM) is a lower bound on the variance of any unbiased estimator. Measuring the pk-pk value of *Y(t)* and subtracting μ_b to satisfy unbiased estimation condition of FIM. (1) can be rewritten as

$$I_b - \mu_b = R \cdot C_b \cdot H(0)_b + n_b - \mu_b \tag{6}$$

where I_b represents pk-pk value of *Y(t)* for b_{th} link.

We are able to simplify (6) as

$$t_b = v_b + w_b \qquad \text{for } b \in \mathcal{B} \tag{7}$$

where

$$t_b = I_b - \mu_b \quad v_b = R \cdot C_b \cdot H(0)_b \quad \omega_b = n_b - \mu_b.$$

The variance of ω_b is equal to the variance of n_b.

The joint probability density function (PDF) of $\{t_b, b \in B\}$ conditioned on θ can be expressed as

$$f_\theta(\mathrm{t}) \propto \prod_{b=1}^{B} \exp\left\{-\frac{1}{2\sigma_{\mathrm{b}}^2}(t_b - v_b)^2\right\} \quad \text{for } b \in \mathcal{B}. \tag{8}$$

This PDF acts an important role in casting the LOS positioning. The FIM is determined by

$$J_\theta = E_\theta\left[\left(\frac{\partial}{\partial\theta}\ln f_\theta(\mathrm{t})\right)\cdot\left(\frac{\partial}{\partial\theta}\ln f_\theta(\mathrm{t})\right)^T\right] \tag{9}$$

which is an $B \times B$ matrix. $E_\theta[\cdot]$ stands for the expectation conditioned on θ. $\hat{\theta}$ denotes an estimate of θ. The CRB is expressed as

$$E_\theta\left[(\hat{\theta}-\theta)\cdot(\hat{\theta}-\theta)^T\right] \geq J_\theta^{-1}. \tag{10}$$

We can get

$$E\left[(\hat{\theta}-\theta)^2\right] \geq \left[J_\theta^{-1}\right]_{bb} \qquad \text{for } 1 \leq b \leq B. \tag{11}$$

According to chain rule, (9) can be decomposed

$$E_\theta\left[\frac{\partial}{\partial\theta}v\frac{\partial}{\partial v}\ln f_\theta(\mathrm{t})\left(\frac{\partial}{\partial\theta}v\cdot\frac{\partial}{\partial v}\ln f_\theta(\mathrm{t})\right)^T\right] = H\cdot J_v\cdot H^T \tag{12}$$

where

$$H = \begin{pmatrix} \dfrac{\partial v_1}{\partial d_1} & \cdots & \dfrac{\partial v_B}{\partial d_1} \\ \vdots & \ddots & \vdots \\ \dfrac{\partial v_1}{\partial d_B} & \cdots & \dfrac{\partial v_B}{\partial d_B} \end{pmatrix}$$

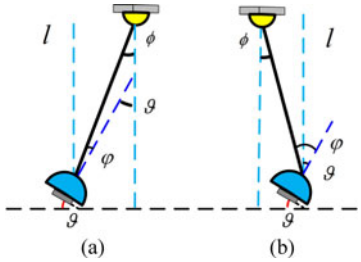

Fig. 1. Two unparallel axis cases.

$$= -\frac{(m+1)(m+3)A_R RC_b h^{m+1}}{2\pi} \times \begin{pmatrix} d_1^{(m+4)} & 0 & 0 \\ 0 & \ddots & 0 \\ 0 & 0 & d_B^{(m+4)} \end{pmatrix}^{-1}$$

is an $B \times B$ matrix. Based on [12],

$$E\left[\left(\frac{\partial}{\partial v}\ln f_\theta(t)\right)\cdot\left(\frac{\partial}{\partial v}\ln f_\theta(t)\right)^T\right] = -E\left(\frac{\partial^2 \ln f_\theta(t)}{\partial v^2}\right) = -\frac{1}{\sigma^2}\left(\frac{\partial v}{\partial v}\right)^2. \quad (13)$$

So

$$J_\nu = \begin{pmatrix} \sigma_1^2 & \cdots & 0 \\ \vdots & \ddots & \vdots \\ 0 & \cdots & \sigma_B^2 \end{pmatrix}^{-1}. \quad (14)$$

We can get

$$J_{d_b}^{-1} = \left(\frac{2\pi d_b^{(m+4)}}{(m+1)(m+3)A_R RC_b h^{m+1}}\right)^2 \sigma_b^2. \quad (15)$$

Based on (11), the CRB on b_{th} distance estimation is

$$\sqrt{\mathrm{var}\left(\widehat{d_b}\right)} \geq \frac{2\pi d_b^{(m+4)}\sigma_b}{(m+1)(m+3)A_R RC_b h^{m+1}}. \quad (16)$$

From (16), we can conclude that if the diffuse channel gain is measured previously in a certain environment and the modulation speed is far less than the channel cutoff frequency, the theoretical accuracy limit of VLC RSSI algorithm is not affected by multipath link.

C. The Influence to CRB of Incidence Angle of Light

Here, we analyze two 2-D cases that the optical axis of LEDs and receivers is not parallel as shown in Fig. 1. φ is not equal to ϕ. ϑ is the angle between detector plane and floor plane.

When LEDs and optical up axis of detector are on the same side of line l, the incidence range is equal to $\vartheta - \phi$. (3) can be expressed as

$$H(f) = \frac{m+1}{2\pi d_b^2}A_R\cos(\vartheta-\phi)\cos^m(\phi) + \frac{A_R}{A_{\mathrm{room}}}\frac{\langle\rho\rangle}{1-\langle\rho\rangle} = \frac{m+1}{2\pi}A_R\frac{\mathrm{h}^m}{d_b^{m+3}}\left(h\cos(\vartheta)+\sqrt{d^2-h^2}\sin(\vartheta)\right) + \frac{A_R}{A_{\mathrm{room}}}\frac{\langle\rho\rangle}{1-\langle\rho\rangle}. \quad (17)$$

Based on (11), the CRB on b_{th} distance estimation is

$$\sqrt{\mathrm{var}\left(\widehat{d_b}\right)} \geq \frac{4\pi d_b^{(m+4)}\sqrt{d_b^2-h^2}\sigma_b}{(m+1)A_R RC_b h^m\,|K_b|} \quad (18)$$

where

$$K_b = d_b^2\sin(\vartheta) - (m+3)\sqrt{d_b^2-h^2} \times\left(\sqrt{d_b^2-h^2}\sin(\vartheta)+h\cos(\vartheta)\right).$$

When LEDs and optical up axis of detector are on the opposite side of line l, the incidence range is equal to $\vartheta + \phi$. (3) can be expressed as

$$H(f) = \frac{m+1}{2\pi d_b^2}A_R\cos(\vartheta+\phi)\cos^m(\phi) + \frac{A_R}{A_{\mathrm{room}}}\frac{\langle\rho\rangle}{1-\langle\rho\rangle} = \frac{m+1}{2\pi}A_R\frac{\mathrm{h}^m}{d_b^{m+3}}\left(h\cos(\vartheta)-\sqrt{d^2-h^2}\sin(\vartheta)\right) + \frac{A_R}{A_{\mathrm{room}}}\frac{\langle\rho\rangle}{1-\langle\rho\rangle}. \quad (19)$$

Similarly, the CRB is

$$\sqrt{\mathrm{var}\left(\widehat{d_b}\right)} \geq \frac{4\pi d_b^{(m+4)}\sqrt{d_b^2-h^2}\sigma_b}{(m+1)A_R RC_b h^m\,|L_b|} \quad (20)$$

where

$$L_b = (m+3)\sqrt{d_b^2-h^2}\left(\sqrt{d_b^2-h^2}\sin(\vartheta)-h\cos(\vartheta)\right) - d_b^2\sin(\vartheta).$$

We can find that (18) and (20) are very complex and ϑ can influence the positioning accuracy. In addition to the above cases, there are other complicated cases in practice. 3-D cases cannot be expressed easily using the CRB. For convenience, we only analyze the usual case that ϑ is zero in simulation part.

III. System Description

In this section, a typical indoor scenario using white lighting LEDs for positioning is described. We adopt frequency division to separate different BSs because it is relatively simple. The frequencies we use to modulate the LEDs are not far from each other. For example, we can use 3, 3.5 and 4 MHz in adjacent three LEDs as shown in Fig. 3. The effect of different attenuation factors caused by different adjacent frequencies can be compensated in the receiver.

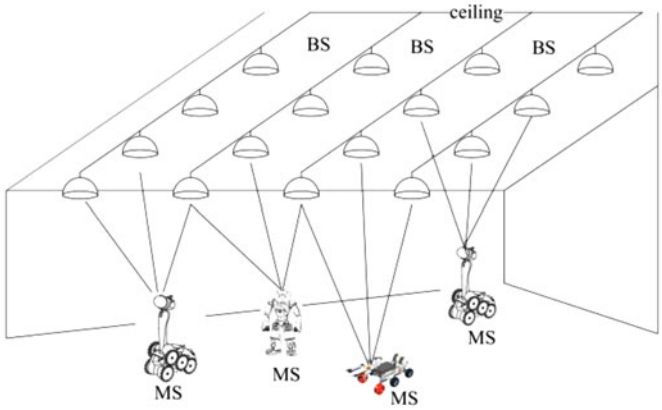

Fig. 2. Schematic diagram of VLC positioning system.

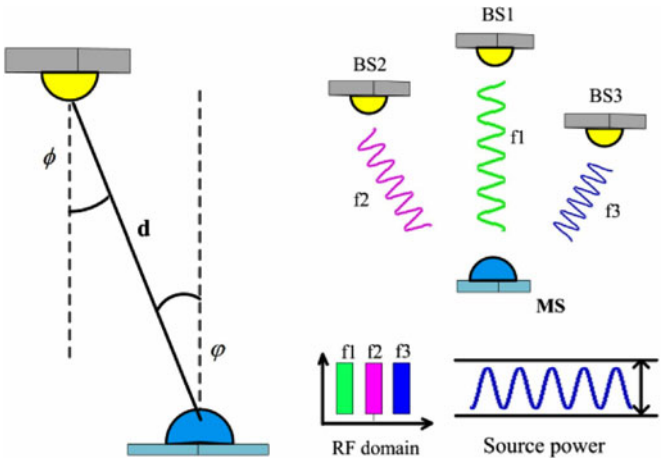

Fig. 3. The diagram of adjacent three LEDs with different frequencies.

A. Noise Model

In the VLC positioning system, the noise is a crucial aspect which could be separated into several parts.

1) Thermal Noise σ_{TH}: The Johnson (thermal) noise is given as [13]

$$\sigma_{TH} = \sqrt{\frac{8\pi\kappa T_e}{G}\eta A_R I_2 \beta^2 + \frac{16\pi^2\kappa T_{\mathrm{e}}\Gamma}{g_m}\eta^2 A_R^2 I_3 \beta^3} \quad (21)$$

where κ is Boltzmann's constant, T_{e} is absolute temperature, G is the open-loop voltage gain, η is the fixed capacitance of photo detector per unit area, Γ is the channel noise factor, β is the equivalent noise bandwidth, g_m is the transconductance and the noise bandwidth factors $I_2 = 0.562$ $I_3 = 0.0868$.

2) Shot Noise From Background Radiation σ_{BG}: The current noise from background radiation is

$$\sigma_{BG} == \sqrt{2qRp_{\mathrm{BS}} A_R \Delta\lambda \beta} \quad (22)$$

where q is the electron charge, p_{BS} is the background spectral irradiance, $\Delta\lambda$ is the bandwidth of the optical filter [13].

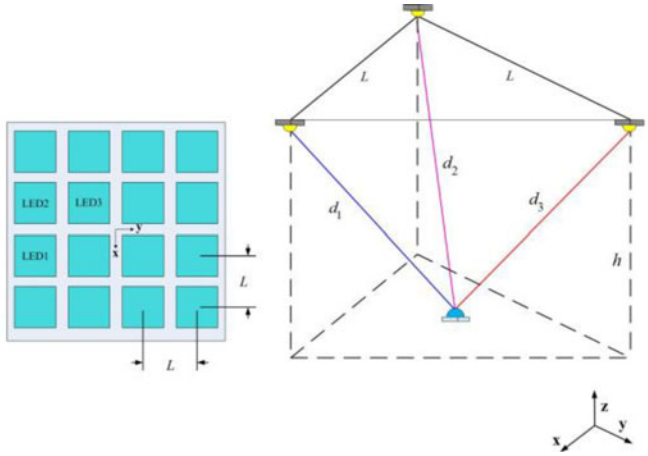

Fig. 4. Square array of LEDs and schematic diagram of VLC positioning.

3) Shot Noise From Received Signal σ_{SS}: The shot noise is given approximately by [14]

$$\sigma_{SS} = \sqrt{2qRP_R\beta} \quad (23)$$

where P_R is pk-pk optical power of the received modulated optical signal in front of the detector.

4) Shot Noise From Dark Current σ_{DC}: The noise from the dark current of photodiode is [14]

$$\sigma_{DC} = \sqrt{2qI_{\mathrm{DC}}\beta} \quad (24)$$

where I_{DC} is the photodiode dark current.

So the variance of Gaussian noise detected by MS is

$$\sigma^2 = \sigma_{DC}^2 + \sigma_{BG}^2 + \sigma_{SS}^2 + \sigma_{TH}^2. \quad (25)$$

B. The Optical Simulation of LEDs Array

A single LED light cannot provide indoor uniform illumination in most of scenarios. It is necessary to get a reasonable layout of LEDs array. In this paper, we assume that the analysis of uniform illumination is based on approximate Lambertian model and each lamp is composed of one LED chip. Since the emitting region area of a LED chip is usually in the level of mm^2 and cm^2, we can treat the LEDs as point sources. The most popular LEDs array is square and triangular.

1) Square LEDs Array: The LED light is incoherent, so it is easy to get the irradiance distribution of numerous BSs. Suppose an array with $N \times M$ LEDs as shown in Fig. 4, irradiance distribution at (x, y, h) is

$$E(x,y,h) = I_0 \sum_{i=1}^{N}\sum_{j=1}^{M}\left[\frac{(m+1)}{2\pi}\cdot\frac{h^{m+1}}{(X^2+Y^2+h^2)^{(m+3)/2}}\right]$$
$$X = x-(N+1-2i)\cdot(L/2) \quad Y = y-(M+1-2j)\cdot(L/2) \quad (26)$$

where I_0 is the luminous intensity, the value of L is the distance between any two lamps, h is the vertical height from BS to MS.

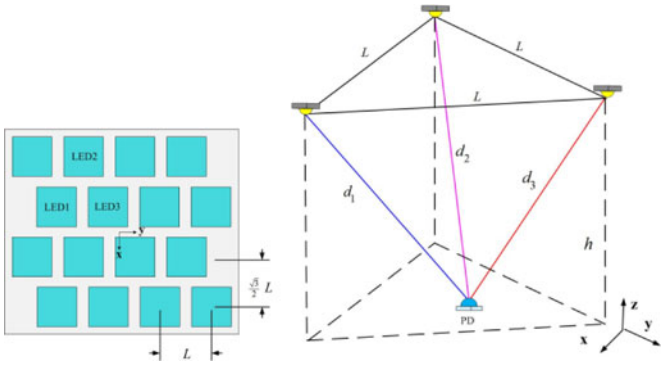

Fig. 5. Triangular array of LEDs and schematic diagram of VLC positioning.

Based on the Sparrow's criterion [15], differentiating E twice, setting $\partial^2 E/\partial x^2 = 0$ at $x = 0$ $y = 0$, and selecting the value of M and N, eventually we can get the maximum value of L determined by the value of h and m.

2) Triangular LEDs Array: Fig. 5 shows the schematic diagram of VLC positioning with triangular array and E is given by the sum of the irradiances for $\{(N \times M) - 0.25\left[2M + (-1)^M - 1\right]\}$ LEDs of an array

$$E(x, y, h) = I_0 \sum_{i=1}^{N} \sum_{j=1}^{M} \left[\frac{(m+1)}{2\pi} \frac{h^{m+1}}{(X^2 + Y^2 + h^2)^{(m+3)/2}} \right]$$
$$X = x - (N_+ - 2i) \cdot (L/2) \quad Y = y - (M + 1 - 2j) \cdot (L/2) \tag{27}$$

where $N_\pm = N + [(-1)j \pm 1]/2$. With the same method, we can get the maximum value of L. In a word, according to the different properties of LEDs, it is necessary to adjust the distance L between any two LEDs to get uniform illumination.

IV. Numerical Results

Some environmental parameters need to be determined, before we analyze the relation between the CRB and some relevant parameters specifically. As shown in Table I, the parameter values we choose are often used in [13], [16], [17].

Based on these values in Table I, we can calculate

$$\sigma_{DC}^2 = 6.4 \times 10^{-22} A^2 \sigma_{BG}^2 = 2.4 \times 10^{-14} A^2$$
$$\sigma_{TH}^2 = 1.1 \times 10^{-13} A^2.$$

However, the shot noise σ_{SS} cannot be calculated before P_R is obtained. Typical LED lights often have values of $m > 30$ [15]. We assume that m is 30, h is 3 m, C is 1W. Then, σ_{SS}^2 is $1.9 \times 10^{-18} A^2$. From these results, we can see the dominant noises in the signal channel of VLC positioning system are thermal noise and shot noise from background radiation.

It is easy to get the accuracy $\sqrt{\mathrm{var}(d_b)} \geq 0.0478$ m. In order to compare this accuracy with RF wireless system, the CRB of RSSI in RF wireless system can be expressed by [9]

$$\sqrt{\mathrm{var}(d_b)} \geq \frac{\ln 10}{10} \cdot \frac{\eta}{\varepsilon} \cdot d \tag{28}$$

where the Gaussian variable is $(0, \eta^2)$, ε is the path loss factor. When we choose the office with soft partition, the parameters will be $\varepsilon = 2.4$ $\eta = 10^{0.96} \approx 9.12$. The estimate distance is still 3 m. The accuracy of RF system is about 2.625 m. Obviously, the accuracy of VLC system is much higher. Especially, we do not consider the pre amplification in this paper. If we add it, the accuracy might be higher.

The nearest three BSs are analyzed based on RSSI algorithm. In the square LEDs array, the value of distance between BS and MS d can be expressed as $d = \sqrt{L^2 + L^2 + h^2}$. (16) can be converted to

$$\sqrt{\mathrm{var}(d_b)} \geq \frac{2\pi(2L^2 + h^2)^{\frac{(m+4)}{2}} \sigma_b}{(m+1)(m+3) A_R R C h^{m+1}}. \tag{29}$$

Similarly, in the triangle LEDs array, the maximum value of d can be expressed as $d = \sqrt{(L/2)^2 + \left(\sqrt{3}L/2\right)^2 + h^2}$

$$\sqrt{\mathrm{var}(d_b)} \geq \frac{2\pi(L^2 + h^2)^{\frac{(m+4)}{2}} \sigma_b}{(m+1)(m+3) A_R R C h^{m+1}}. \tag{30}$$

In the following analysis, if there is no special instruction, the analysis is based on the square LEDs array and L represents the maximum value of distances between lamps in different LEDs array. Since the influence to CRB of source pk-pk power is similar with detector area and responsivity, only the variations of C is considered from 0.2 to 1 W. Other two parameters are treated as constant.

TABLE I
Some Typical Parameter Values

Symbol	Quantity	Value Unit
q	electron charge	1.6×10^{-19} C
I_{DC}	dark current	5 pA
Γ	channel noise factor	1.5
R	detector responsivity	0.4 A/W
β	equivalent noise bandwidth	400 MHz
G	open-loop voltage gain	10
κ	Boltzmann's constant	1.38×10^{-23}
T_e	absolute temperature	300 K
A_R	detector effective area	0.2 cm^2
g_m	transconductance	30 m/s
$\Delta\lambda$	bandwidth of the optical filter	400 (380–780) nm
p_{BS}	background spectral irradiance	5.8×10^{-6} $\mathrm{W/cm}^2 \cdot \mathrm{nm}$
η	fixed capacitance of photo detector	112 $\mathrm{pF/cm}^2$

A. The Influence to the CRB of h

In the analysis above, we found the range of L is determined by the LEDs layout. When we adopt the square LEDs of 10×10 and m of 30, it is easy to get the maximum value of L under different values of h. In Fig. 6 the CRB is plotted versus source pk-pk optical power. The height of room h varies from 1.5 to 3 m. The CRB drops with the decreasing of h. In other words, the distance from the MS to BS is shorter, the positioning accuracy

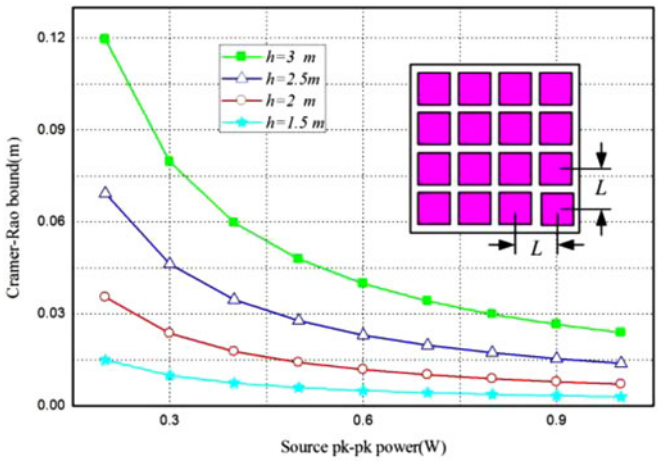

Fig. 6. CRB versus source optical pk-pk power with various heights.

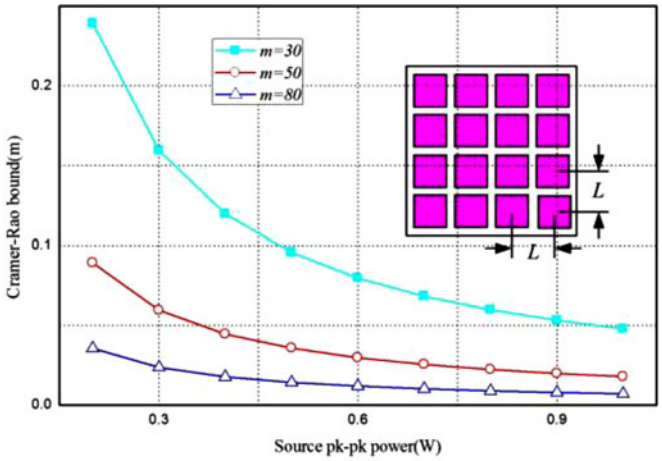

Fig. 7. CRB versus source optical pk-pk power with the number of *m*.

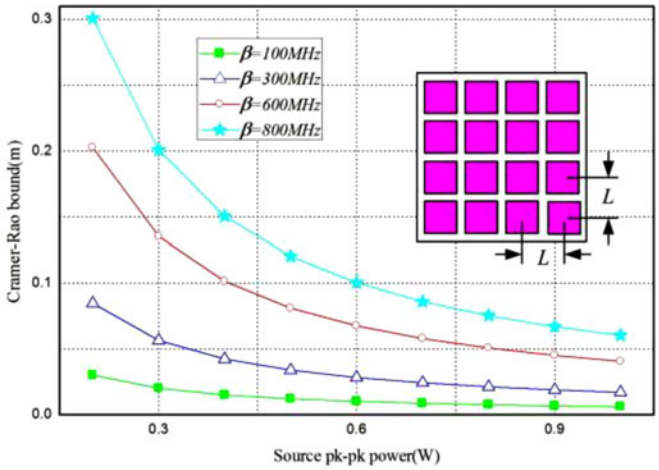

Fig. 8. CRB versus source pk-pk optical power with various equivalent noise bandwidths.

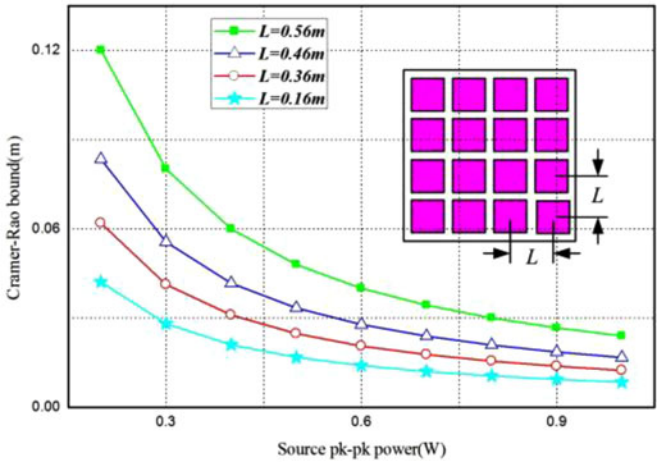

Fig. 9. CRB versus source pk-pk optical power with various LEDs space.

is higher. The result is consistent with the fact. When the source pk-pk optical power is 1 W with the height of room 3 m, the CRB is less than 3 cm.

B. The Influence to the CRB of m

In practical applications, the radiation model of LEDs is not perfect Lambertian distribution and *m* might be different in different LED manufacturers. We vary the value of *m* from 30 to 80. The vertical height *h* is set as 3 m. It is noted that value of *L* is mutative with *m*. In Fig. 7, we find that the CRB drops with the increasing of *m*, which is caused by the definition of *m*. The value of *m* can be expressed as $m = -\ln 2 / \ln(\theta_{1/2})$, where $\theta_{1/2}$ is defined as the view angle when irradiance is half of the value at 0°. When the value of *m* increases, it means the value of $\theta_{1/2}$ decreases. The signal is more concentrated and the signal-to-noise ratio (SNR) is higher. Therefore, the accuracy is higher.

C. The Influence to the CRB of β

The equivalent noise bandwidth β presents the effect of transmitter, receiver and electric circuit. In Fig. 8, the CRB is plotted versus pk-pk optical power with equivalent noise bandwidth from 100 to 800 MHz. The CRB rises with increasing of equivalent noise bandwidth because there is much more noise with large equivalent noise bandwidth, whereas the bandwidth of signal is limited. For pk-pk optical power of 1 W and equivalent noise bandwidth of 800 MHz, the CRB is about 6 cm.

D. The Influence to the CRB of L

Finally, we analyze the CRB with various LEDs space *L*. The height of room is 3 m and *m* is 30. According to Sparrow's criterion, the maximum value of *L* is 0.56 m in square LEDs array. We vary *L* from 0.16 to 0.56 m. The CRB drops with the decreasing of *L* in Fig. 9, although larger value of *L* means bigger area of uniform illumination. It may be explained that the signal is relatively weak with the increasing of *L*.

The analysis of CRB in triangle LEDs array is in the same way of square LEDs array. We assume the parameter values of triangle LEDs array and square LEDs array are identical. In order to compare the value of CRB in different LEDs array, we adopt the same range of *L* from 0.16 to 0.56 m. The Fig. 10 shows the CRB of triangle LEDs array. When *L* is 0.56 m, the

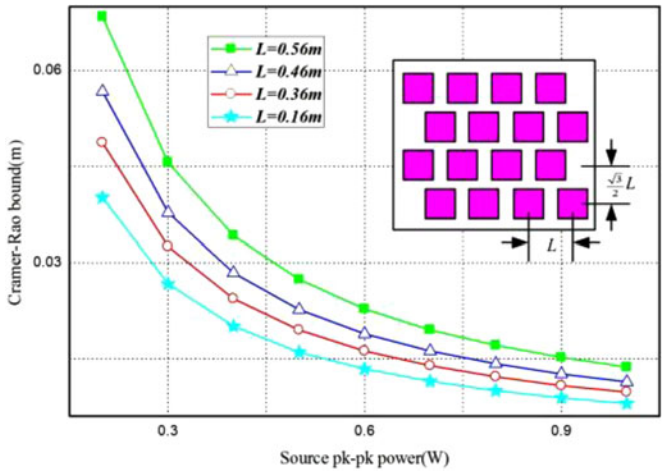

Fig. 10. CRB versus source optical pk-pk power with various LEDs space in triangle array.

CRB is less than 7 cm. It is 5 cm less than the CRB of the square LEDs with same parameters. Therefore, considering the positioning accuracy, the layout of triangle LEDs is better than square LEDs in VLC positioning system.

V. Conclusion

In this paper, we derive the CRB model of VLC system based on RSSI algorithm. The influence to CRB of multipath reflections can be ignored when diffuse channel gain is measured previously in a certain environment and the modulation speed is far less than the channel cutoff frequency. Two simple cases where optical axis of LEDs and detectors are not parallel are discussed. Depending on LEDs array, we discuss the impact of some important parameters to the CRB in detail. The results show that the RSSI positioning accuracy with the triangle LEDs is higher than that with the square LEDs. The theoretical accuracy of VLC positioning system depends on the layout of LEDs, the receiver circuit, incidence angle of light, LED light source and photodiode. The CRB in the level of centimeters could be achieved with typical parameter values. This gives a significant prospect for accurate indoor positioning application based on VLC RSSI scheme.

In future works, the comparison of VLC positioning accuracy based on different algorithms is planned. In addition, the further detailed research of influences to CRB of multipath reflections and incidence angle will be a priority.

References

[1] T. Taguchi, "Technological innovation of high-brightness light emitting diodes (LEDs) and a view of white LED lighting system," *Optronics*, vol. 19, no. 228, pp. 113–119, 2000.

[2] T. Tamura, T. Setomoto, and T. Taguchi, "Fundamental characteristics of the illuminating light source using white LED based on InGaN semiconductors," *IEE Trans. Jpn.*, vol. l20-A, no. 2, pp. 244–249, 2000.

[3] X. H. Liu, H. Makino, and Y. Maeda, "Basic study on indoor location estimation using visible light communication platform," in *Proc. IEEE 30th Annu. Int. Eng. Med. Biol. Soc.*, Vancouver, BC, Canada, Aug. 2008, pp. 2377–2380.

[4] Y. Tanaka, T. Komine, S. Haruyama, and M. Nakagawa, "Indoor visible communication utilizing plural white LEDs as lighting," in *Proc. 12th IEEE Int. Symp. Personal, Indoor Mobile Radio Commun.*, San Diego, CA, USA, 2001, pp. F81–F85,

[5] S. H. Yang, E. M. Jung, and S. K. Han, "Indoor location estimation based on LED visible light communication using multiple optical receivers," *IEEE Commun. Lett.*, vol. 17, no. 9, pp. 1834–1837, Sep. 2013.

[6] T. Q. Wang, Y. A. Sekercioglu, A. Neild *et al.*, "Position accuracy of time-of-arrival based ranging using visible light with application in indoor localization systems," *J. Lightw.Technol.*, vol. 31, no. 20, pp. 3302–3308, Oct. 2013.

[7] L. Huang and C. C. Ko, "Performance of maximum-likelihood channel estimator for UWB communications," *IEEE Commun. Lett.*, vol. 8, no. 6, pp. 356–358, Jun. 2004.

[8] A. L. Deleuze, C. J. Le Martret, P. Ciblat, and E. Serpedin, "Cramer–Rao bound for channel parameters in ultra-wide band based system," in *Proc. IEEE Workshop Signal Process. Adv. Wireless Commun.*, Lisbon, Portugal, 2004, pp. 140–144.

[9] Y. H. Qi, "Wireless geolocation in a non-line-of-sight environment," Ph.D. dissertation, Dept. Elect. Eng., , Princeton Univ., Princeton, NJ, USA, 2003.

[10] V. Jungnickel, V. Pohl, S. Nonning, and C.V. Helmolt, "A physical model of the wireless infrared communication channel," *IEEE J. Sel. Areas Commun.*, vol. 20, no. 3, pp. 631–640, Apr. 2002.

[11] K. Lee and H. Park, "Channel model and modulation schemes for visible light communication," in *Proc. IEEE 54th Int. Midwest Symp. Circuits Syst.*, 2011, pp. 1–4.

[12] S. M. Kay, "Cramer–Rao lower bound," in *Fundamentals of Statistical Signal Processing: Estimation Theory*, San Francisco, CA USA: Pearson Education Education, 2001.

[13] T. Komine and M. Nakagawa, "Fundamental analysis for visible-light communication system using LED lights," *IEEE Trans. Consumer Electron.*, vol. 50, no. 1, pp. 100–107, Feb. 2004.

[14] H. Manor and S. Arnon, "Performance of an optical wireless communication system as a function of wavelength," *Appl. Opt.*, vol. 42, no. 21, pp. 4285–4294, Jul. 2003.

[15] I. Moreno, M. Avendano-Alejo, and R. I. Tzonchev, "Designing LED arrays for uniform near-field irradiance," *Appl. Opt.*, vol. 45, no. 10, pp. 2265–2272, Apr. 2006.

[16] T. Komine and M. Nakagawa, "Performance evaluation on visible-light wireless communication system using white LED lightings," in *Proc. 9th IEEE Symp. Comput. Commun.*, 2004, pp. 258–263.

[17] T. Komine, J. H. Lee, S. Haruyama, and M. Nakagawa, "Adaptive equalization system for visible light wireless communication utilizing multiple white LED lighting equipment," *IEEE Trans. Wireless Commun.*, vol. 8, no. 6, pp. 2892–2900, Jun. 2009.

Xueli Zhang received the B.E. degree from the Changchun University of Science and Technoloy, Changchun, China, in 2012. From 2013, she studied in Changchun University of Science and Technoloy and the Optoelectronic System Laboratory, Institute of Semiconductors, Chinese Academy of Sciences. Her research interests include visible light communication and optics.

Jingyuan Duan received the Ph.D. degree from the Beijing University of Aeronautics and Astronautics, Beijing, China, in 2008. From 2008, he joined the Institute of Semiconductor, CAS in Chinese Academy of Sciences and later became an Associate Professor. His research interests include visible light communications and its applications. He has chaired and participated in the Natural Science Foundation, important projects in Chinese Academy of Sciences, etc.

Yuegang Fu research interests include advanced optical testing technology and biomimetic optical aspects.

Ancun Shi received the M.E. degree in communication and information system from the North China Electric Power University, Beijing, China, in 2009. From 2009, he joined the Institute of Semiconductor, CAS in Chinese Academy of Sciences. His research interests include visible light communications and its applications.